RESEARCH ARTICLE | AUGUST 23 2024

### Laser induced fluorescence using frequency modulated light



Special Collection: Proceedings of the 25th Topical Conference on High-Temperature Plasma Diagnostics

E. E. Scime D; J. Freeze; T. J. Gilbert ; T. E. Steinberger



Rev. Sci. Instrum. 95, 083550 (2024) https://doi.org/10.1063/5.0219309





#### Articles You May Be Interested In

Continuous wave cavity ring-down spectroscopy for velocity distribution measurements in plasma

Rev. Sci. Instrum. (October 2015)

Minimum ion-beam exposure-dose determination for chemically amplified resist from printed dot matrices

J. Vac. Sci. Technol. B (November 1999)

Improving pulsed laser induced fluorescence distribution function analysis through matched filter signal processing

Rev. Sci. Instrum. (August 2024)





## Laser induced fluorescence using frequency modulated light

Cite as: Rev. Sci. Instrum. 95, 083550 (2024); doi: 10.1063/5.0219309

Submitted: 16 May 2024 • Accepted: 9 August 2024 •

**Published Online: 23 August 2024** 











E. E. Scime, De J. Freeze, T. J. Gilbert, De and T. E. Steinberger

#### **AFFILIATIONS**

Department of Physics and Astronomy, West Virginia University, Morgantown, West Virginia 26506, USA

Note: This paper is part of the Special Topic on Proceedings of the 25th Topical Conference on High-Temperature Plasma Diagnostics.

a) Author to whom correspondence should be addressed: escime@wvu.edu

#### **ABSTRACT**

The small signal-to-noise ratio (SNR) of conventional laser induced fluorescence (LIF) measurements using a continuous wave laser, either diode or dye, is typically overcome by amplitude modulating the laser at a specific frequency and then using lock-in amplification to extract the signal from measurement noise. Here, we present LIF measurements of the neutral helium velocity distribution function in an rf plasma using frequency modulated (FM) laser injection. A pulse train of 100% amplitude modulation is generated synthetically with a random sequence of pulse lengths. The FM signal then drives an acoustic optic modulator placed in the path of the injection beam in an LIF measurement. The signal from a fast photomultiplier tube is digitized and cross-correlated with the known modulation signal. The resultant FM-based LIF signal outperforms a conventional lock-in-based LIF measurement on the same plasma in terms of SNR and precision.

Published under an exclusive license by AIP Publishing. https://doi.org/10.1063/5.0219309

#### I. INTRODUCTION

Laser induced fluorescence (LIF) is a powerful tool for plasma diagnosis since it is able to non-perturbatively measure the spatially resolved velocity distribution function (VDF) of a target species. LIF is accomplished by optically pumping a target electronic state and measuring the resultant fluorescent emission. If a wide-linewidth laser is used, the measurement is proportional to the density of the target electronic state. If a tunable narrowlinewidth laser is used (narrower than the absorption linewidth of the target electronic state), measurements of the fluorescent emission as a function of laser wavelength yield a measurement of the Doppler shifted absorption linewidth, which is directly relatable to the VDF of the target species. Variations of LIF systems deployed on plasma experiments are plentiful and include simple singlepoint LIF measurements,2 multiplexed LIF,3 planar LIF,4 threedimensional LIF,5 and time-resolved LIF.6 Typical LIF measurements have velocity resolutions of ~ 50 m/s and temperature resolutions of  $\delta T/T \sim 0.1$ . Spatial resolutions of  $\ll 1 \text{ mm}^3$  are routinely

In most implementations of LIF in plasmas, weak fluorescent signal is discriminated against spontaneously generated background

light by external modulation of a continuous-wave (CW) laser beam and subsequent phase synchronous detection, or by using pulsed lasers to greatly increase the fluorescent signal. Phase synchronous detection, usually accomplished with a lock-in amplifier, has been key to LIF measurements in plasmas with CW lasers. In use for nearly 100 years, a lock-in amplifier essentially multiplies a noisy signal that contains an embedded signal of interest at a specific frequency with another sinusoidal function of a reference frequency, producing two AC signals of half amplitude at the difference and sum frequencies of the multiplied signals that are then passed through a low-pass filter. If the frequencies of the signals are different, the result is zero. If signal and reference frequencies are the same, the lock-in output is a DC signal proportional to the signal amplitude. By using the reference signal to modulate the output of a laser, e.g., with an optical modulator, and measuring the modulated fluorescent emission, the amplitude of the LIF emission at the modulation frequency is recovered. To reduce the effects of noise, the modulation signal is often in the kHz to MHz range to take advantage of the 1/f noise spectrum in most experimental systems. The low-pass filter results in a slow response to changes in the signal and when the spontaneous plasma emission varies on this time scale, significant oscillations in the resultant lock-in signal may occur.

While employing a very narrow modulation frequency has the advantage of being able to focus signal recovery on a very narrow region of the frequency spectrum of the target signal, the information content of a fixed sinusoidal frequency is zero. If, instead, the LIF emission was modulated in a manner to maximize the information content in the modulation, the likelihood of random noise generating the same modulation pattern would be effectively zero. Encoding the laser amplitude with a white noise spectrum would maximize the information content of the modulation. Such a signal recovery approach is often referred to as a matched filter analysis. Matched filter analysis has been used in a variety of fields, e.g., telecommunications, radar, and the detection of gravitational waves, to improve the processed signal-to-noise (SNR) of time series measurements at times corresponding to a known signal.<sup>7,8</sup> Given a known signal template present within additive stochastic noise, matched filter analysis maximizes the SNR of the measurement and improves detection thresholds.

In this work, we report a comparison of LIF measurements in a helium plasma obtained with standard lock-in analysis using sinusoidal laser amplitude modulation and those obtained using a random pattern of frequency modulation (near white noise) of the laser amplitude for which the signal was then extracted from the measured fluorescent emission using matched filter analysis. The advent of fast signal processing electronics with a large bit-depth (12-bit or better) has enabled this alternate approach. We find that the random frequency modulated (FM) method yields better SNR and is more robust to naturally occurring low frequency oscillations in the spontaneous plasma emission.

#### II. EXPERIMENTAL SYSTEM AND ANALYSIS METHOD

The experimental measurements reported here were performed in the Compact Helicon for Waves and Instabilities Experiment (CHEWIE). Plasma is generated in CHEWIE by driving a double loop m=0 antenna at an rf power of 500 W, a magnetic field of 720 G, and a fill pressure of 7.1 mTorr. Helium gas is fed into the end of a Pyrex tube (D=6 cm, L=60 cm) through a mass-flow controller and the plasma is confined by four water-cooled electromagnetic coils.

For neutral helium velocity distribution function (VDF) measurements, a Sirah Matisse ring dye laser is tuned to 587.7249 nm (vacuum wavelength) to pump the He I  $2p^3P_1^o$  metastable state and to observe the resulting 388.9750 nm (vacuum wavelength) fluorescence after collisional transfer from the  $3d^3D_2$  state to  $3p^3P_2^o$  and then relaxation to the  $2s^3S_1$  state. As the laser frequency is swept over 10 GHz, the fluorescent emission from the excited state is amplified with a bandpass-filtered (1 nm bandwidth) narrowband, high-gain, Hamamatsu photomultiplier tube (PMT).

The laser light was injected along the axial magnetic field through a linear polarizer, followed by a quarter waveplate to select a single circular polarization. The circularly polarized light yields a single peak VDF from the  $\Delta m = \pm 1$  Zeeman-split cluster. The laser output of ~1 W passes through an acousto-optic modulator and is then single-mode fiber coupled and injected into the CHEWIE plasma. The layout of the LIF system is shown in Fig. 1. Helium neutral LIF was selected for these preliminary measurements because the 587 nm transition is an exceptionally strong transition, and past LIF studies in He I resulted in excellent signal to noise.

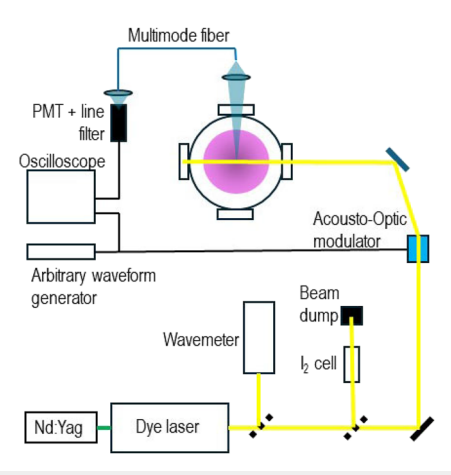


FIG. 1. Apparatus used for the frequency modulated LIF measurements. Tunable laser light is produced by a Sirah Matisse ring dye laser that is pumped with a 10 W CW Nd:YAG laser. Small fractions of the output laser light are used for wavelength measurements with an angstrom UVII WS6-200 wavelength meter and a molecular iodine cell. The bulk of the laser light passes through an acousto-optic modulator (AOM) with a modulation pattern created with an arbitrary waveform generator. The fluorescent emission is collected perpendicular to the injected beam and transported by a multi-mode optical fiber to a bandpass-filtered PMT detector with a 20 kHz bandwidth whose time series output is recorded with an oscilloscope. In the standard lock-in method, the AOM is replaced with an optical chopper and the waveform generator is replaced with a lock-in amplifier.

The matched filter analysis process<sup>11</sup> begins with a measured signal M(t) over a time interval  $t_1 \le t \le t_2$  at discrete time steps spaced by  $\Delta t$  and a reference signal R(t) over the time interval  $t_1 + T \le t \le t_2 + T$  using the same discrete time step  $\Delta t$ . T is a time offset that is chosen to ensure the reference signal pulse fits within the measurement time interval. The measured and reference signals (measured at discrete time steps) are indexed with an integer n such that M(t) = M(n) and R(t + T) = R(n), where n is an integer in the range  $0 \le n \le N - 1$ , and  $N = (t_2 - t_1)/\Delta t$ .

The matched filter output S(x), where x is an integer in the range  $1 \le x \le 2N - 1$ , is the convolution of the measured signal and the reversed reference signal R(x - n) summed over all elements of n,

$$S(x) = \sum_{n=0}^{N-1} R(x-n)M(n).$$
 (1)

The maximum strength of the LIF signal embedded in the time series occurs at a time of N+L, where L is the offset, in time steps between the reference signal and the measured signal. The time offset between the measured and reference signals is determined by defining S(N) as t=0, with  $(x-N)\Delta t$  defining a new x axis. If the maximum occurs at L=0, reference and measured signals are perfectly aligned in their respective time series. In the case of CW LIF, the reference signal is repeated over time, resulting in a series of local maxima.

To maximize the effect of the modulation on the LIF emission intensity, the modulation pattern sent to the acousto-optic modulator consisted of a series of variable length, variable delay pulses of 100% modulation amplitude, i.e., a pulse width modulated signal with non-repeating intervals between pulses. The modulation pattern was created digitally and uploaded to a Rigol DG 1022 arbitrary waveform generator that provided the input for an Intra-Action ATM-803DA1 acousto-optic modulator. Figure 2(a) shows an expanded view of a portion of the pulse pattern developed for these experiments. To produce the frequency modulated pattern, we started with a 100 Hz square-wave with a 10 ms record length, such that there were equal total intervals of "on" and "off" times as used in the comparison lock-in-based measurements. The square-wave was then divided into 0.01 ms sections and randomly rearranged, resulting in a series of square pulses of random lengths and random intervals with a minimum of 0.01 ms for both length and interval. The pattern was then repeated to form the total modulation waveform.

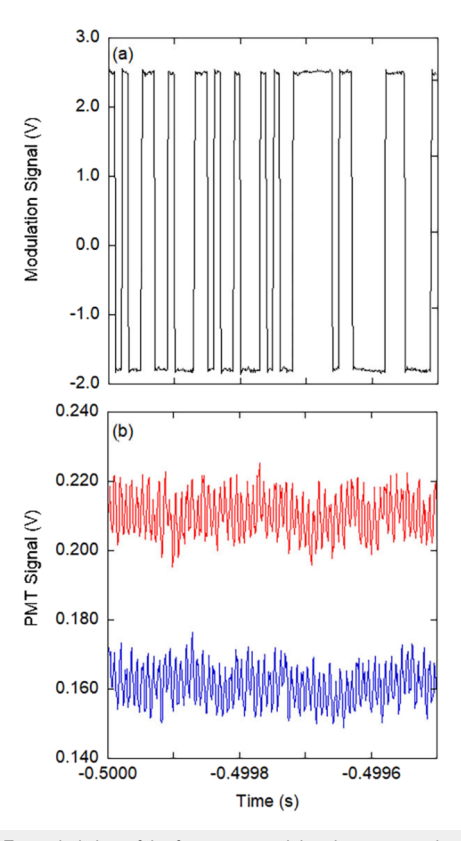
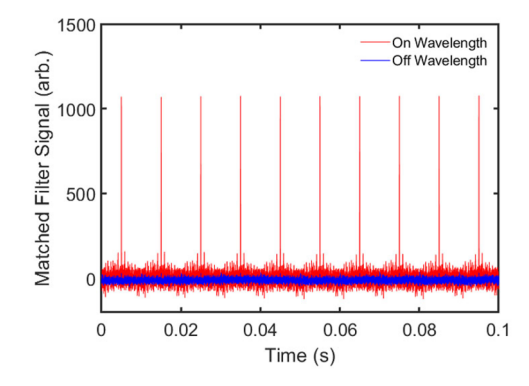


FIG. 2. (a) Expanded view of the frequency modulated pattern used to encode the laser amplitude. The pattern was created from a series of square wave pulses of random lengths and random intervals with a minimum of 0.01 ms for both length and interval. This pattern was continuously repeated. 0.5 ms of the pattern is shown here. The fluctuations in the maximum and minimum amplitudes reflect the bit resolution of the arbitrary waveform generator and the resolution of the oscilloscope used for the measurements. (b) The portion of the time series of the PMT signal corresponding to the modulation pattern shown in panel (a). Two PMT signals are shown: when the laser is tuned to the center of the absorption line (red) and when the laser is tuned away from the center of the absorption line (blue). The two signals have been offset artificially in voltage so that both traces are easily viewed.

#### III. RESULTS

An example of the output of the PMT while the laser is being modulated is shown in Fig. 2(b). Two PMT traces are shown: when the laser wavelength was tuned to the peak of the absorption line (red) and when the laser wavelength was tuned away from the peak of the absorption line. Neither of the PMT trace shows any obvious modulation in synch with the modulation waveform. The PMT output was recorded for one second and then processed as described in Eq. (1). Over the 2 s timescale, we observed a slow variation in the overall signal level in the PMT signal amplitude. When using a lockin amplifier with a time constant on the order of one second, such an oscillation will cause a slow variation in the measured lock-in amplitude. Figure 3 shows two results of processed time series measurements for frequency modulated (FM) laser output. The analysis period (100 ms) spans multiple repetitions of the modulation pattern. The first measurement, shown in red, was obtained when the laser wavelength was tuned to the peak of the absorption line. The second measurement, shown in blue, is for the laser tuned to a wavelength outside of the absorption line shape. There are two important features shown in Fig. 3. First, the average value of the processed signal (averaged over 100 ms) for the laser tuned off of the line is zero. Second, the amplitudes of the repeating peaks in the processed signal are remarkably consistent. In fact, there is little to no variation in the amplitude of the peaks. This is a result of the statistical likelihood of the modulation pattern accidentally appearing in the PMT output being effectively zero.

These measurements were repeated for a range of laser wavelengths that spanned the Doppler broadened neutral helium absorption line. The laser was moved to each new wavelength and a one second time series was recorded before moving to the next wavelength. We then repeated the measurements for the exact same plasma conditions, but with the standard lock-in based measurement method. For the lock-in method, a single 5 kHz square-wave signal generated from the frequency generator was sent to the acousto-optic modulator. The time constant on a SRS 830 lock-in was set to one second with an 18 dB/octave roll off. The lock-in output was sent to the oscilloscope and recorded at each wavelength for



**FIG. 3.** Expanded view (100 ms of the full 1 s time series) of the cross correlation of the PMT signal and the frequency modulated waveform when (red) the laser is tuned at the center of the absorption line and (blue) when the laser is tuned to a wavelength outside of the absorption line shape. The individual peaks provide the magnitude of the LIF signal embedded in the PMT time series.

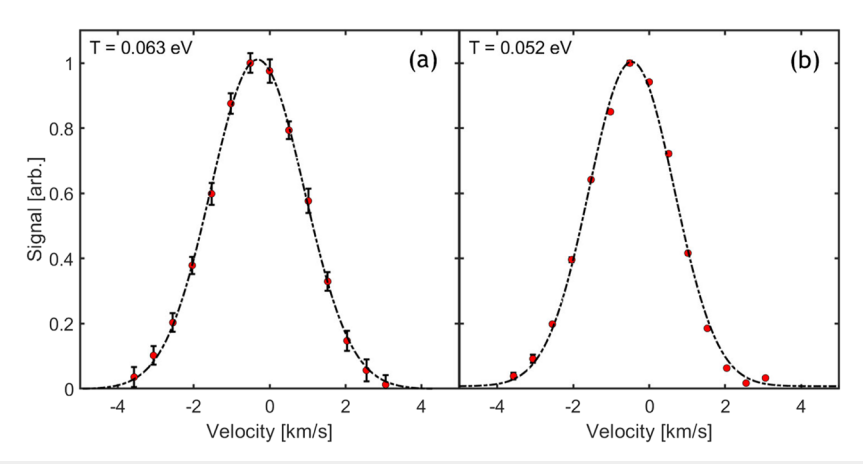


FIG. 4. Measured LIF emission amplitude (points) as a function of neutral atom velocity (laser wavelength) using (a) square-wave modulation and a lock-in amplifier and (b) frequency modulation, followed by a matched filter cross-correlation analysis. Maxwellian velocity distribution fits to both measurements (solid line) are also shown.

two seconds before the laser was stepped to the next wavelength. The lock-in was allowed time to settle to the new signal level at each new wavelength before each measurement of the lock-in output. Figure 4 shows the results of both measurements. The lock-in method measurement, Fig. 4(a), has excellent SNR with modest errors in each emission measurement. The FM method, Fig. 4(b), yields a slightly narrower measurement in velocity space, and the errors in each measurement are noticeably smaller than for the lock-in method. For the FM method, the errors in each measurement point were determined from the standard deviation of the amplitudes of all the peaks in the processed measurements. For the lock-in method, half of the total fluctuation in the output signal around the mean output over the 2 s measurement interval was used for the errors at each wavelength. At the peak of the absorption line, the relative error in the FM method is 0.4%, whereas in the lock-in method, the relative error at the same wavelength was 6%—an order of magnitude larger.

Each neutral VDF was fit with the expression,

$$I(\nu) = \alpha + \beta \exp\left(-\frac{(\nu - \nu_o - \nu_D)^2}{2\sigma^2}\right),\tag{2}$$

where I(v) is the intensity of the fluorescent signal as a function of the laser frequency v;  $\alpha$  is the background intensity;  $\beta$  is the maximum signal amplitude;  $\sigma$  is the standard deviation of the distribution;  $v_o$  is the rest frame frequency of the transition; and  $v_D$  is the mean frequency of the fit to the absorbed photons relative to the rest frame frequency of the transition. The drift velocity of the bulk population is obtained from  $v_D = U_D v_o/c$ , where  $U_D$  is the drift velocity and c is the speed of light. The temperature is derived from the standard deviation  $\sigma = \sqrt{eTv_o^2/2mc^2}$ , where e is the electron charge, T is the temperature in eV, and m is the mass of the atom or ion in kg. For these plasma conditions and magnetic fields, Stark broadening, pressure broadening, and Zeeman splitting are all ignorable and the absorption linewidth is dominated by the thermal Doppler broadening from the motion of the

neutral atoms. The laser linewidth,  ${\sim}100$  MHz, is much smaller than the measured absorption linewidth. For the lock-in method, the measured temperature is  $0.063 \pm 0.009$  eV. For the FM method, the measured neutral temperature is  $0.056 \pm 0.001$  eV. The FM measurement lies within the error bounds of the lock-in method, but is considerably more precise. Room temperature in these units is 0.026 eV, so the measured neutral helium temperature is consistent with the neutrals in this discharge being heated slightly by collisions and cooled through equilibration with the walls of the vacuum chamber.

#### **IV. CONCLUSIONS**

These measurements demonstrate that it is possible to use frequency modulation encoding of an injected laser to improve upon the signal recovery results obtained with classic lock-in amplification in a laser induced fluorescence measurement. Increased SNR with this method is easily obtained by using longer modulation patterns and acquiring the time series for a longer time period. Effectively, this method encrypts the laser signal and looks for the specific encryption pattern in the PMT time series. With improved bit-depth in the measurement apparatus, the dynamic range of this method will also increase, i.e., even very small signals will be recoverable.

#### **ACKNOWLEDGMENTS**

The authors thank Professor Fred Skiff of the University of Iowa for valuable discussions about this method. This work was supported by NSF Award No. 1902111.

#### **AUTHOR DECLARATIONS**

#### **Conflict of Interest**

The authors have no conflicts to disclose.

# 03 July 2025 14:31:0°

#### **Author Contributions**

E. E. Scime: Conceptualization (lead); Formal analysis (equal); Funding acquisition (lead); Methodology (lead); Project administration (lead); Resources (lead); Supervision (lead); Writing – original draft (lead); Writing – review & editing (lead). J. Freeze: Investigation (supporting); Software (supporting). T. J. Gilbert: Data curation (equal); Formal analysis (equal); Investigation (equal); Software (equal); Writing – original draft (equal). T. E. Steinberger: Formal analysis (equal); Investigation (equal); Software (equal); Supervision (equal); Writing – original draft (equal).

#### **DATA AVAILABILITY**

The data that support the findings of this study are available from the corresponding author upon reasonable request.

#### **REFERENCES**

- <sup>1</sup>R. A. Stern and J. A. Johnson, Phys. Rev. Lett. **34**, 1548 (1975).
- <sup>2</sup>E. E. Scime, P. A. Keiter, M. W. Zintl, M. M. Balkey, J. L. Kline, and M. E. Koepke, Plasma Sources Sci. Technol. 7, 186 (1998).
- <sup>3</sup>A. K. Hansen, M. Galante, D. McCarren, S. Sears, and E. E. Scime, Rev. Sci. Instrum. 81, 10D701 (2010).
- <sup>4</sup>M. C. Paul and E. E. Scime, Rev. Sci. Instrum. **92**, 043532 (2021).
- <sup>5</sup>D. S. Thompson, R. Khaziev, M. Fortney-Henriquez, S. Keniley, E. E. Scime, and D. Curreli, Phys. Plasmas **27**, 073511 (2020).
- <sup>6</sup>E. Scime, C. Biloiu, C. Compton, F. Doss, D. Venture, J. Heard, E. Choueiri, and R. Spektor, Rev. Sci. Instrum. **76**, 026107 (2005).
- <sup>7</sup>F. Acernese, F. Barone, R. D. Rosa, A. Eleuteri, S. Pardi, L. Milano, and G. Russo, Classical Quant. Grav. 21, S1849 (2004).
- <sup>8</sup>T. J. Gilbert, T. E. Steinberger, and E. E. Scime, Rev. Sci. Instrum. **95**, 083521 (2024).
- J. S. McKee, E. E. Scime, I. Arnold, and S. Loch, Phys. Plasmas 28, 022108 (2021).
  E. Scime, R. Hardin, C. Biloiu, A. M. Keesee, and X. Sun, Phys. Plasmas 14, 043505 (2007).
- <sup>11</sup>S. E. Bialkowski, Appl. Spectrosc. **42**, 807 (1988).